The impact of Al_2O_3 back interface layer on low-temperature growth of ultrathin Cu(In,Ga)Se_2 solar cells*

LIU Yang (刘杨)[1], **LIU Wei** (刘玮)[1]**, **CHEN Meng-xin** (陈梦馨)[2], **SHI Si-han** (史思涵)[1], **HE Zhi-chao** (何志超)[1], **GONG Jin-long** (巩金龙)[2], **WANG Tuo** (王拓)[2], **ZHOU Zhi-qiang** (周志强)[1], **LIU Fang-fang** (刘芳芳)[1], **SUN Yun** (孙云)[1], **and XU Shu** (徐术)[3]

1. *Tianjin Key Laboratory of Thin Film Devices and Technology, Institute of Photoelectronic Thin Film Devices and Technology, Nankai University, Tianjin 300071, China*
2. *Key Laboratory for Green Chemical Technology of Ministry of Education, Collaborative Innovation Center of Chemical Science and Engineering (Tianjin), School of Chemical Engineering and Technology, Tianjin University, Tianjin 300072, China*
3. *Davidson School of Chemical Engineering, Purdue University, West Lafayette IN47907, USA*

(Received 12 March 2018; Revised 22 March 2018)

With reducing the absorber layer thickness and processing temperature, the recombination at the back interface is severe, which both can result in the decrease of open-circuit voltage and fill factor. In this paper, we prepare Al_2O_3 by atomic layer deposition (ALD), and investigate the effect of its thickness on the performance of Cu(In,Ga)Se_2 (CIGS) solar cell. The device recombination activation energy (E_A) is increased from 1.04 eV to 1.11 eV when the thickness of Al_2O_3 is varied from 0 nm to 1 nm, and the height of back barrier is decreased from 48.54 meV to 38.05 meV. An efficiency of 11.57 % is achieved with 0.88-μm-thick CIGS absorber layer.

Document code: A **Article ID:** 1673-1905(2018)05-0363-4

DOI https://doi.org/10.1007/s11801-018-8036-7

Cu(In,Ga)Se_2 (CIGS) has reached an efficiency of 22.9% so far[1], indicating a matured laboratorial technology. Considering the application of CIGS solar cells in industry, the production costs play an important role due to the scarcity of In[2]. Therefore, some groups have focused on the researches of reducing CIGS absorber layer thickness to submicron even less (the standard CIGS absorber layer thickness is 2.0—3.0 μm). What is more, the CIGS absorber layers can be prepared with lower processing temperature, which can also reduce the wear of equipment.

Though the aforementioned solutions could reduce the production costs and improve the yield, there are many problems in the practical production. The light absorption is insufficient in thinner CIGS absorber layer, and this may cause smaller short-circuit current density (J_{sc})[3]. Except for the light loss, the electrical loss in ultrathin CIGS devices is also severe. The electron-hole pairs are separated with the help of built-in electric field in space charge region (SCR), but the width of SCR is smaller in the device with thinner CIGS absorber layer, so it is easier for photoelectrons to diffuse to the back electrode. As a result, the recombination at the back interface is severe[4,5]. The high-temperature processes are favorable for the formation of $MoSe_2$, and it can decrease the height of the back barrier, making the contact of Mo and CIGS from Schottky contact to ohmic contact[6]. Reducing the deposition temperature would impede the formation of $MoSe_2$ and further bring about the severe recombination in the back interface[7-9]. Therefore, the recombination in the back interface is more serious when the ultrathin CIGS absorber layers are prepared in low-temperature processes.

In this paper, we prepare Al_2O_3 film by atomic layer deposition (ALD) and employ it into low-temperature growth of ultrathin CIGS solar cells. We mainly focus on the passivation effect of Al_2O_3 film, and further ascertain the optimum thickness of Al_2O_3 acting as the back interface layer.

The Al_2O_3 films are deposited on metal Mo by ALD, and the thicknesses of Al_2O_3 are 0 nm, 1 nm and 2 nm, respectively. Then the Al_2O_3 films are annealed in vacuum chamber, and the anneal temperature is 400 °C, which is nearly the same as the deposition temperature of

* This work has been supported by the National Natural Science Foundation of China (Nos.61774089 and 61504067), and the Yang Fan Innovative & Entrepreneurial Research Team Project (No.2014YT02N037).

** E-mail: wwl@nankai.edu.cn

CIGS absorber layer. The CIGS absorber layers are processed by three-stage co-evaporation based on the Al_2O_3 films, and the deposition temperature is below 450 °C. The thicknesses of CIGS absorber layers are about 0.9 μm.

We implement X-ray diffraction (XRD) measurements on the CIGS films, and the results are shown in Fig.1. The Al_2O_3 films do not alter the preferred orientation of CIGS absorber layer, and it is still (112). But the crystallization intensity is increased when the thickness of Al_2O_3 is 1 nm. The surface scanning electron microscope (SEM) images of metal Mo coated by Al_2O_3 films with varied thicknesses are displayed in Fig.2. The surface of metal Mo becomes denser with the increase of thickness of Al_2O_3. Compact Mo surface is favorable for the (112) preferred orientation of CIGS absorber layer[10]. But the Al_2O_3 back interface layer is a barrier for the sodium diffusion, 2 nm is too thick to let enough sodium diffuse into CIGS absorber layer. Appropriate content of sodium in CIGS absorber layer can promote the crystallization of (112)[11-13], so the crystallization intensity of CIGS absorber layer with 2-nm-thick Al_2O_3 is inferior as shown in the XRD measurement results.

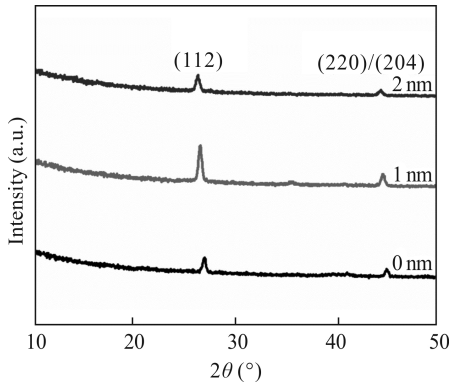

Fig.1 The XRD patterns of CIGS absorber layers with different thicknesses of Al_2O_3 films

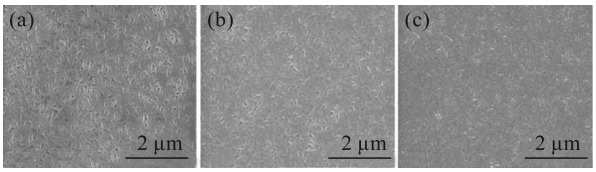

Fig.2 The surface SEM images for Mo coated by Al_2O_3 films with different thicknesses of (a) 0 nm, (b) 1 nm and (c) 2 nm

To explore the impacts of Al_2O_3 films thicknesses on the morphology of CIGS absorber layer, we further carry out cross-section SEM measurements on the CIGS absorber layers, and the results are shown in Fig.3. The grain sizes are larger in CIGS absorber layer with 1-nm-thick Al_2O_3 films acting as back interface layer, and this provides a possibility of the reduced recombination in the CIGS bulk. However, the grain size of CIGS absorber in Fig.3(c) is smaller than that in Fig.3(b), which may be related to the variation of sodium content as discussed above.

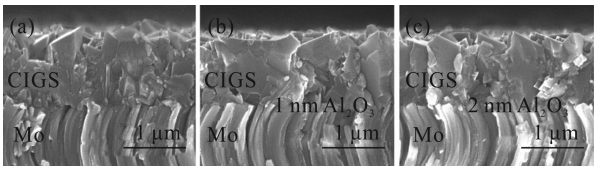

Fig.3 The cross-section SEM images for CIGS absorber layers with different thicknesses of Al_2O_3 films of (a) 0 nm, (b) 1 nm and (c) 2 nm

The current density-voltage (*J-V*) curves of completed devices based on the above CIGS absorber layers are shown in Fig.4, and the specific electrical parameters are listed in the insert table. The improvements of V_{oc} and *FF* are nearly 20 mV and 12%, respectively, both of which contribute to the increase of efficiency. The efficiency can reach 11.57 % with 1-nm-thick Al_2O_3 acting as back interface layer. The improved V_{oc} and *FF* are benefitted from the decreased recombination in the CIGS absorber layer as well as the back interface, and this will be verified later. Due to the aforementioned detriments caused by thick Al_2O_3 films, the device performance is poorer than the others.

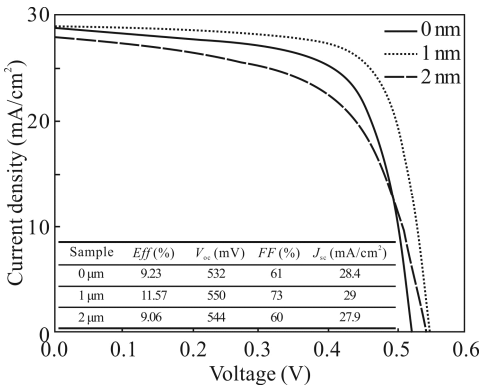

Fig.4 The *J-V* curves for devices with different thicknesses of Al_2O_3 films (The insert table shows the specific electrical parameters of each cell.)

In order to prove the passivation effects of Al_2O_3 films with different thicknesses, the external quantum efficiency (*EQE*) measurements are executed, and the results are displayed in Fig.5. The *EQE* in 600—800 nm are improved obviously in devices with Al_2O_3 films. Under the influence of Al_2O_3 films, the crystallization of CIGS absorber is better (as shown in Fig.1), and the grain size is larger (as shown in Fig.3) compared with the reference sample, so the recombination occurring in the CIGS absorber layer is reduced, and the loss of photo-generated current is lesser, so the *EQE* response are higher.

Different from the *EQE* in the range of 600—800 nm, the *EQE* in 800—1 100 nm show another variation. The

EQE of the device with 1-nm-thick Al_2O_3 film is higher than that of a reference cell, indicating the passivation effect of Al_2O_3 film. The negative fixed charges density in the annealed Al_2O_3 film is relatively high, and this is favorable for the formation of built-in electric field, which prevents the diffusion of electrons to back interface and reduces the recombination at the back interface. Except for the field-effect passivation, the chemical passivation is another advantage of Al_2O_3 film due to the low interface-trap charge density[14,15]. While the *EQE* response begins to drop when the thickness of Al_2O_3 film increases. This is related to the high resistance of Al_2O_3 films. The films processed by ALD are compact, and the resistance is increased with the increase of thickness of Al_2O_3 film. The resistance introduced by 2-nm-thick Al_2O_3 film is so large that the *EQE* in long-wavelength region is lower.

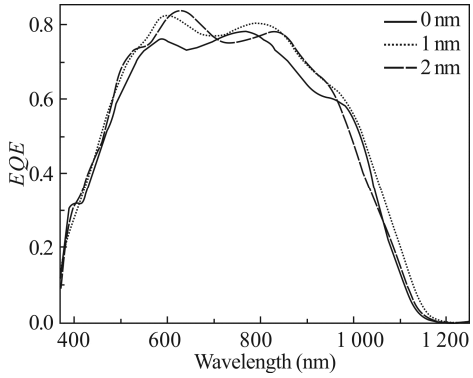

Fig.5 The *EQE* curves for devices with different thicknesses of Al_2O_3 films

Temperature dependent *J-V* measurements are performed to explore the impacts of Al_2O_3 back interface layers in detail. We can fit temperature dependence of V_{oc} and obtain the device recombination activation energy (E_A) according to the equation as[16]

$$V_{oc} = \frac{E_A}{q} - \frac{AKT}{q} \times \ln\left(\frac{J_{00}}{J_L}\right), \quad (1)$$

where A, J_{00} and J_L are diode factor, diode reverse saturation current pre-factor and photocurrent, respectively. For three samples with different thicknesses from 0 nm to 2 nm, E_A values are 1.04 eV, 1.11 eV and 1.07 eV, respectively, as shown in Fig.6(a). The larger E_A represents less interface recombination, and it indicates the main recombination occurs in the SCR[17]. What is more, 1 nm is the optimum thickness for Al_2O_3 film acting as back interface in our experiments. Thicker Al_2O_3 films will introduce larger resistance, and this will lead to a larger back barrier height. We obtain the back barrier height through fitting the series resistance according to the following equation as[18]

$$R_S = R_0 + \frac{k}{qA^*T} \times e^{\frac{\Phi_B}{kT}}, \quad (2)$$

where A^* is Richardson constant, Φ_B is the height of back barrier, R_0 is the background series resistance of front contact and absorber layer bulk resistance, and R_0 is small enough which can be ignored. As shown in Fig.6(b), the height of back barrier is 39.79 meV in the device with 2-nm-thick Al_2O_3 back interface layer. And the data on the ordinate are larger than the others, indicating the series resistances are larger as well, which consists with the previous description. Besides, 1-nm-thick Al_2O_3 back interface layer can not only restrain the recombination but also reduce the back barrier height.

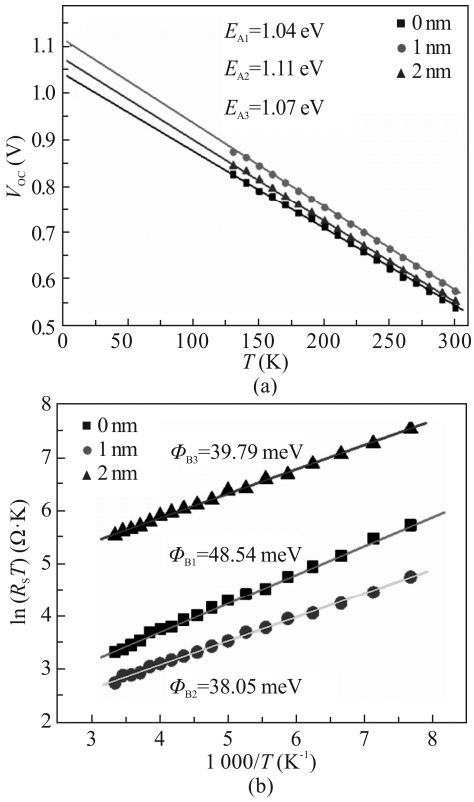

Fig.6 (a) The temperature dependent V_{oc} and (b) back barrier height for devices with different thicknesses of Al_2O_3 films

In conclusion, Al_2O_3 back interface layer with appropriate thickness can improve the crystal qualities of absorber layers and device performance. For the device with 1-nm-thick Al_2O_3 film, the achieved efficiency and *EQE* are both the highest. E_A of the device with Al_2O_3 is increased, and the height of back barrier is reduced from 48.54 meV to 38.05 meV when the thickness of Al_2O_3 is varied from 0 nm to 1 nm. But the device performance is deteriorated due to the high resistance of Al_2O_3 when the thickness of Al_2O_3 is 2 nm. Therefore, 1 nm is the optimum thickness for Al_2O_3 acting as back interface layer in low-temperature growth of ultrathin CIGS solar cells. Finally for the device with 1-nm-thick Al_2O_3, the conversion efficiency of 11.57% is achieved based on 0.88-μm-thick CIGS absorber layer prepared by the low-temperature processes below of 450 °C.

References

[1] Solar Frontier Achieves World Record Thin-Film Solar Cell Efficiency of 22.9%, http://www.solar-frontier.com/eng/news/2017/1220_press.html.

[2] M. Gloeckler and J.R. Sites, J. Appl. Phys. **98**, 103703 (2005).

[3] N. Amin, P. Chelvanathan, M.I. Hossain and K. Sopian, Energy Procedia. **15**, 291(2012).

[4] P. Reinhard, F. Pianezzi, L. Kranz, S. Nishiwaki, A.Chirila, S. Buecheler and A.N. Tiwati, Prog. Photovolt: Res. Appl. **23**, 281 (2015).

[5] E. Jarzembowski, B. Fuhrmann, H. Leipner, W. Franzel and R. Scheer, Thin Solid Films **633**, 61 (2017).

[6] E. Jarzembowski, F. Syrowatka, K. Kaufmann, W. Franzel, T. Holscher and R. Scheer, Appl. Phys. Lett. **107**, 051601 (2015).

[7] J.H. Yoon, J.H. Kim, W.M. Kim, J.K. Park, Y.J. Baik, T.Y. Seong and J.H. Jeong, Prog. Photovolt: Res. Appl. **22**, 90 (2014).

[8] R. Caballero, M. Nichterwitz, A. Steigert, A. Eicke, I. Lauermann, H.W. Schock and C.A. Kaufmann, Acta Mater. **63**, 54 (2014).

[9] X.L. Zhu, Z. Zhou, Y.M. Wang, L. Zhang, A.M. Li and F.Q. Huang, Sol. Energy Mater. Sol. Cells **101**, 57 (2012).

[10] J.H. Yoon, W.M. Kim, J.K. Park, Y.J. Baik, T.Y. Seong and J.H. Jeong, Prog. Photovolt: Res. Appl. **22**, 69 (2014).

[11] P. Jackson, R. Wuerz, D. Hariskos, E. Lotter, W. Witte and M. Powalla, Phys. Status Solidi (RRL)-Rapid Res. Lett. **10**, 583 (2016).

[12] J.H. Yoon, T.Y. Seong and J.H. Jeong, Prog. Photovolt: Res. Appl. **21**, 58 (2013).

[13] K. Granath, M. Bodegard and L. Stolt. Huang, Sol. Energy Mater. Sol. Cells **60**, 279 (2000).

[14] J. Joel, B. Vermang, J. Larsen, O.D. Gargand and M. Edoff, Phys. Status Solidi RRL **9**, 288 (2015).

[15] B. Vermang, J.T. Watigen, V. Fjallstrom, F. Rostvall, M. Edoff, R. Kotipalli, F. Henry and D. Flandre, Prog. Photovolt: Res. Appl. **22**, 1023 (2014).

[16] V. Nadenau, U. Rau, A. Jasenek and H.W. Schock, J. Appl. Phys. **87**, 584 (2000).

[17] T. Mise, S. Tajima, T. Fukano, K. Higuchi, T. Wasgio, K. Jimbo and H. Katagiri, Prog. Photovolt: Res. Appl. **24**, 1009 (2016).

[18] S.S. Hegedus and W.N. Shafarman, Prog. Photovolt: Res. Appl. **12**, 155 (2004).